Drift-wave turbulence and zonal flow generation

R. Balescu
Physique Statistique–Plasmas, Association Euratom-Etat Belge, Université Libre de Bruxelles, Campus Plaine, Boulevard du Triomphe, 1050 Bruxelles, Belgium

(Received 29 May 2003; published 29 October 2003)

Drift-wave turbulence in a plasma is analyzed on the basis of the wave Liouville equation, describing the evolution of the distribution function of wave packets (quasiparticles) characterized by position **x** and wave vector **k**. A closed kinetic equation is derived for the ensemble-averaged part of this function by the methods of nonequilibrium statistical mechanics. It has the form of a non-Markovian advection-diffusion equation describing coupled diffusion processes in **x** and **k** spaces. General forms of the diffusion coefficients are obtained in terms of Lagrangian velocity correlations. The latter are calculated in the decorrelation trajectory approximation, a method recently developed for an accurate measure of the important trapping phenomena of particles in the rugged electrostatic potential. The analysis of individual decorrelation trajectories provides an illustration of the fragmentation of drift-wave structures in the radial direction and the generation of long-wavelength structures in the poloidal direction that are identified as zonal flows.

DOI: 10.1103/PhysRevE.68.046409 PACS number(s): 52.35.Ra, 52.25.Gj, 52.35.Mw, 52.35.Kt

I. QUALITATIVE OVERLOOK

In the quest for controlled nuclear fusion, the main problem is the confinement of plasma by means of a magnetic field for a time sufficient for the start of the nuclear reactions. For this reason, an understanding of the particle and energy cross-field transport is crucial for the control of unfavorable losses. The main mechanism of these losses appears to be the anomalous transport produced by drift-wave turbulence, due to the unavoidable gradients of temperature and pressure present in the confinement devices (such as the tokamak) [1,2]. For many years, progress has stumbled on the understanding and control of this loss mechanism.

An important breakthrough was the discovery of the so-called *H mode* (or high-confinement mode) operation regime of the tokamak [3], which led to a substantial improvement in the confinement time. The explanation of this effect is the formation of a *transport barrier* at a certain distance from the center of the magnetic axis. At this barrier, the turbulence level propagating from the core is substantially reduced. As a result, the transport processes are also reduced, leading to the observed increase in the confinement time. Clearly, this experimental discovery triggered an intense effort in experimental, computational, and theoretical plasma physics in order to understand the possible mechanisms of the transition to the *H* mode. An enormous amount of literature has appeared in the past 20 years: a very clear review, together with an extensive list of references (prior to 2000) will be found in Ref. [4]. A grouping of more recent results will be found in Ref. [5]. The aspects related to the *H*-mode bifurcation are covered in the review paper [4], and more extensively in the works of Itoh and Itoh and their co-workers [6–8]. We now outline the general ideas of the production of transport barriers.

Consider a magnetized plasma (in a constant magnetic field **B**) in a state of drift-wave turbulence [4]. The electrostatic potential, as well as related quantities, have a rugged spatial structure which is, moreover, continuously changing in time. Suppose that in a certain region there exists a systematic *shear flow* in the direction perpendicular to the magnetic field and to the gradients (i.e., the poloidal direction in a tokamak), which we first assume to be stationary. This flow will carry along *nonuniformly* the drift-wave structures, thus deforming them. After some time the structure is torn up and fragmented into smaller substructures. This means that the various regions of the initial structure lose their correlation because of the drag by the shear flow. As a result, *an overall decrease of the correlation length is produced in the direction perpendicular to the shear flow*.

In a real situation, as encountered in a tokamak (but also in the terrestrial atmosphere), the situation is more complex. It will be shown that under certain circumstances, the drift-wave turbulence is able to generate spontaneously a shear flow. The latter is also random, but characterized by a correlation length that is much longer than that of the original drift-wave turbulence. This large-scale turbulent poloidal flow is called a *zonal flow*. Its effect is again, understandably, a tearing apart of the drift-wave structures and their fragmentation. This effect is very strikingly seen in the massively parallel numerical simulations published in Ref. [9]. The most elaborate explanation of this effect was initiated by Diamond and his collaborators [10,11] (see also [12]) and is still being actively pursued (see, e.g., [5,13–16]).

In the present paper, we are mainly interested in the mechanism of generation of the zonal flows. The "classical" discussion of this problem is exposed in Ref. [13] and in Sec. A.i. of Ref. [5]. Its argument can be summarized as follows. The fragmentation produced by the complex zonal flows results in an *increase* of the mean square of the radial wave vector $\langle k_r^2\rangle$, which is a measure of the inverse square of the correlation length λ_r^{-2} in the radial direction (i.e., the direction of the density gradient). As a result, the drift-wave frequency $\omega_d(\mathbf{k})=k_yV_*/(1+\rho_s^2k^2)$ will *decrease*. (Here $V_*=\rho_s c_s/L_n$ is the electron diamagnetic velocity, ρ_s the electron Larmor radius, c_s the ion-acoustic velocity, L_n the density gradient length, and k_y is the component of the wave vector **k** in the y direction, mimicking the poloidal component k_θ in a tokamak, $k^2=k_r^2+k_\theta^2$; for simplicity, the temperature is assumed constant.) It follows from the conservation of the "action density" $\tilde{N}(\mathbf{k})=\varepsilon(\mathbf{k})/\omega_d(\mathbf{k})$ that the drift-wave energy $\varepsilon_{\mathbf{k}}$ must also decrease, it being transferred to the large-scale zonal flow energy. We are thus in the presence of an instability that produces an inverse cascade in **k** space. After its saturation, a new state appears, in which the level of small-scale turbulence, hence the anomalous radial transport, is significantly reduced: a *transport barrier* has been created.

This semiqualitative argument has a weak point, because $\tilde{N}(\mathbf{k})$ is not quite the conserved action density, as shown by some of the authors of [5,13] in Ref. [14]. In subsequent calculations, however, the equation of evolution of the correct action density (see below) is used. A diffusion coefficient in **k** space is derived from the latter in Refs. [13], [5] by using "the methodology of quasilinear theory." The action thus presumably obeys a diffusion equation (which is not written down), explaining the growth of $\langle k_r^2\rangle$ and the decrease of the radial drift-wave transport.

The authors of Refs. [13], [5] correctly note that this quasilinear treatment of **k**-space diffusion is of limited validity. When the turbulence level is not very weak, new features become important. The rugged fluctuating potential landscape (as it appears in the numerical simulations of Ref. [9]) produces transient *trapping of the particle trajectories* in its troughs or around its peaks, as well as formation of coherent structures [17,18]. The difficult nonlinear treatment of these processes has been approached in various ways in the recent literature.

In Ref. [14], the "wave kinetic equation" is treated by a multiple-time perturbation technique which in first approximation yields the quasilinear result. In the next approximation, the resulting equation admits localized solutions of the kink-soliton type. Such coherent structures are supposed to be actors in nonlocal transport schemes based on the avalanche concept from self-organized criticality theory [5,15]. As the avalanches are random events, it appears that transport in such conditions is intermittent, and the heat flux must be treated statistically in this framework. Its variance (estimated in [5]) may provide a measure of these fluctuations.

Coherent nonlinear structures that are exact solutions of a model system of one-dimensional equations for the drift-wave–zonal flow system are very elegantly determined in Ref. [16]. These correspond to wave trapping, which finally produces solitons, shocks, or other similar localized structures. These may be responsible for some of the non-Gaussian features of transport mentioned above.

In the present paper, we take a different approach to the interpretation of the trapping effect on the global transport. We base our treatment on the decorrelation trajectory (DCT) method, introduced and developed in several works, starting in 1998 [19–21], and extended here in order to include the random walk in **k** space. The basic idea is to decompose the global ensemble of realizations of the fluctuating potential into subensembles. Each of the latter comprises the set of all realizations having a fixed initial value of the potential and of its first two derivatives. A particle (or a wave packet) moving in different subensembles has different trajectories because it is trapped in different regions and at different times. A deterministic "decorrelation trajectory" is determined as the average trajectory in a given subensemble. The Lagrangian velocity correlations, hence the diffusion coefficients, are then calculated as weighted superpositions of Eulerian velocity correlations in all subensembles, evaluated along these deterministic DCT's.

The DCT approximation is one significant step beyond the well-known Corrsin approximation [22], which includes the quasilinear and the Bohm approximations. General expressions of the running diffusion coefficients are derived in the DCT framework; explicit results depend, however, on the statistical definition of the potential, which must be specified *a priori*. As is the case with all theories of strong turbulence, it is impossible to give a specific validity criterion of the approximation involved in the DCT method. Its validity can only be assessed by *a posteriori* comparison with experiment or simulations. It may be stated here that the first application of the method to electrostatic turbulence [19], i.e., its prediction of the shape of the radial diffusion coefficient curve, agrees quite well with numerical simulations [23].

The fate of the amplified zonal flows and the final stabilization of the turbulence is much less understood. Several interpretations have been advanced but no final conclusion seems to appear yet. This matter will not be discussed in the present paper.

The paper is organized as follows. In Sec. II, the exact starting point of the theory is defined, in the form of a Liouville equation for the wave action density, i.e., the distribution function of drift-wave packets or "quasiparticles." In Sec. III, an application of the methods of nonequilibrium statistical mechanics leads in full generality to a nondiffusive equation, containing in principle the non-Gaussian effects mentioned above. A "local approximation" produces a closed non-Markovian advection-diffusion equation for the ensemble average of the distribution function, i.e., a kinetic equation. The latter describes two *coupled* diffusive processes in position space and in wave-vector space. General expressions for the diffusion tensors are derived in terms of Lagrangian velocity correlation functions. The latter are evaluated in Sec. IV by applying the decorrelation trajectory method. Although their numerical evaluation is left for a forthcoming paper, the mechanism of the trapping processes and the generation of zonal flows are vividly apparent from an analysis of individual decorrelation trajectories, performed in Sec. V. Section VI contains a comparison with Refs. [5], [13], and conclusions are given in Sec. VII.

II. THE WAVE LIOUVILLE EQUATION

We consider a plasma in the presence of a strong magnetic field (such as a tokamak). Locally this magnetic field can be considered as constant, equal to **B**. A Cartesian reference system is then defined by three unit vectors: $\mathbf{e}_z$ directed along **B**, $\mathbf{e}_x$ in the direction of the density gradient (the temperature is taken constant, for simplicity), mimicking the radial direction in a tokamak, and $\mathbf{e}_y=\mathbf{e}_z\times\mathbf{e}_x$, representing the poloidal direction (shearless slab geometry). If **B** is sufficiently strong, the collisionless motion of the particles can be approximated by the quasi-two-dimensional motion of their guiding centers, characterized by their position vector $\mathbf{x} = (x,y)$.

The plasma is assumed to be in a turbulent state produced by drift waves. In many interesting situations the spectrum of the electrostatic potential fluctuations, ϕ, contains two widely separated peaks, corresponding, respectively, to long-range fluctuations and to short-range fluctuations. The fluctuating potential can thus be represented as a sum of a long-range part $\bar{\phi}$ and a short-range part $\tilde{\phi}$: $\phi = \bar{\phi} + \tilde{\phi}$. These are most easily identified in Fourier space:

$$\bar{\phi}(\mathbf{q},t) = (2\pi)^{-2} \int d\mathbf{x}\, e^{i\mathbf{q}\cdot\mathbf{x}} \bar{\phi}(\mathbf{x},t), \quad \rho_s q \ll 1,$$

$$\tilde{\phi}(\mathbf{k},t) = (2\pi)^{-2} \int d\mathbf{x}\, e^{i\mathbf{k}\cdot\mathbf{x}} \tilde{\phi}(\mathbf{x},t), \quad \rho_s k \ll 1. \tag{1}$$

Whenever such a significant separation exists between short and long scales, a *partial average* operation $\langle\, \rangle_\sim$ can be introduced, defined as an ensemble average over small-scale quantities. Thus, in particular,

$$\bar{\phi} = \langle \phi \rangle_\sim, \quad \langle \bar{\phi} \rangle_\sim = \bar{\phi}, \quad \langle \tilde{\phi} \rangle_\sim = 0. \tag{2}$$

The small-scale potential fluctuation $\tilde{\phi}$ never appears isolated in the expressions of the macroscopic, observable quantities; the interesting quantities are quadratic functionals of the potential. Of particular importance is the *action density* $N(\mathbf{x},\mathbf{k},t)$, which is a conserved quantity. Its definition, in the case of drift waves, is somewhat subtle [14]. Calling $\hat{\phi}(\mathbf{k},t) = (1+\rho_s^2 k^2)\tilde{\phi}(\mathbf{k},t)$, the action density is defined as

$$N(\mathbf{x},\mathbf{k},t) = \int d\mathbf{p}\, e^{i\mathbf{p}\cdot\mathbf{x}} \langle \hat{\phi}_{\mathbf{k}} \hat{\phi}_{-\mathbf{k}+\mathbf{p}} \rangle_\sim, \quad \rho_s p \ll 1. \tag{3}$$

This quantity obeys an equation of evolution derived in Ref. [14],

$$\partial_t N(\mathbf{x},\mathbf{k},t) = \frac{\partial H(\mathbf{x},\mathbf{k},t)}{\partial \mathbf{x}} \cdot \frac{\partial N(\mathbf{x},\mathbf{k},t)}{\partial \mathbf{k}} - \frac{\partial H(\mathbf{x},\mathbf{k},t)}{\partial \mathbf{k}} \cdot \frac{\partial N(\mathbf{x},\mathbf{k},t)}{\partial \mathbf{x}}, \tag{4}$$

where

$$H(\mathbf{x},\mathbf{k},t) = \omega_d(\mathbf{k}) + \mathbf{k}\cdot \bar{\mathbf{V}}(\mathbf{x},t), \tag{5}$$

and $\bar{\mathbf{V}} = (c/B)\,(\mathbf{e}_z \times \nabla \bar{\phi})$ is the long-range part of the electric drift velocity. The remarkable feature here is the Hamiltonian structure of the evolution of a set of "quasiparticles," i.e., wave packets, characterized by the canonically conjugate variables $(\mathbf{x},\mathbf{k})$ [24,25]. The action density plays the role of the phase-space distribution of the quasiparticles, and obeys the Liouville equation (4), which can be written in terms of a Liouville operator $\mathcal{L}_W$, defined as in statistical mechanics by the Poisson bracket of H and N:

$$\partial_t N = \mathcal{L}_W N \equiv [H,N]. \tag{6}$$

Equation (4) is usually called the wave kinetic equation in the literature. From the viewpoint of statistical mechanics, this is an inappropriate name (see the next section). It will rather be called the *wave Liouville equation*.

III. THE WAVE KINETIC EQUATION

Given the Hamiltonian structure of Eq. (6), it is natural to treat this equation by the methods of nonequilibrium statistical mechanics [26] in order to derive a true wave kinetic equation. The procedure is a generalization of the work of Ref. [27]. We note that the action density is the result of a *partial averaging* over the small-scale fluctuations. It remains, however, a fluctuating quantity in the large-scale domain; indeed, the Hamiltonian contains the fluctuating term $\mathbf{k}\cdot\bar{\mathbf{V}}(\mathbf{x},t)$. Hence the wave Liouville equation is a *stochastic differential equation*, i.e., it is of the same nature as a *hybrid kinetic equation* [28]. The associated characteristic equations are therefore typical *V Langevin equations*.

The first step in the treatment of the wave Liouville equation is to separate an average part and a fluctuating part in the distribution function:

$$N(\mathbf{x},\mathbf{k},t) = n(\mathbf{x},\mathbf{k},t) + \delta N(\mathbf{x},\mathbf{k},t),$$

$$n(\mathbf{x},\mathbf{k},t) = \langle N(\mathbf{x},\mathbf{k},t)\rangle, \quad \langle \delta N(\mathbf{x},\mathbf{k},t)\rangle = 0. \tag{7}$$

Note that the average here is over the large-scale potential fluctuations. We also decompose the wave Liouvillian operator as

$$\mathcal{L}_W = \mathcal{L}_W^0 + \delta\mathcal{L}_W, \tag{8}$$

where

$$\mathcal{L}_W^0 = -\mathbf{V}^g(\mathbf{k}) \cdot \frac{\partial}{\partial \mathbf{x}}, \tag{9}$$

$$\delta\mathcal{L}_W = -\bar{\mathbf{V}}(\mathbf{x},t)\cdot \frac{\partial}{\partial \mathbf{x}} - \bar{\mathbf{W}}(\mathbf{x},\mathbf{k},t)\cdot \frac{\partial}{\partial \mathbf{k}}. \tag{10}$$

Here $\mathbf{V}^g(\mathbf{k})$ is the (unperturbed) group velocity of the drift waves,

$$\mathbf{V}^g(\mathbf{k}) = \frac{\partial \omega_d(\mathbf{k})}{\partial \mathbf{k}} = \frac{V_*}{(1+\rho_s^2 k^2)^2}\{-2\rho_s^2 k_x k_y \mathbf{e}_x + [1+\rho_s^2(k_x^2 - k_y^2)]\mathbf{e}_y\}. \tag{11}$$

It represents the velocity of propagation of the wave packet, or quasiparticle, in the absence of turbulence. We assume it to be independent of $\mathbf{x}$, i.e., the density gradient (hence V_*) is treated locally as a constant: In Eq. (10) a shorthand notation was introduced for the fluctuating "velocity" of the wave vector,

$$\overline{\mathbf{W}}(\mathbf{x},\mathbf{k},t)=-\frac{\partial}{\partial\mathbf{x}}[\mathbf{k}\cdot\overline{\mathbf{V}}(\mathbf{x},t)]. \tag{12}$$

Averaging the wave Liouville equation (4) we obtain [omitting a term $\langle\delta\mathcal{L}_W\delta N\rangle$ in Eq. (14), which does not contribute to Eq. (13)]

$$\partial_t n-\mathcal{L}_W^0 n=\langle\delta\mathcal{L}_W\delta N\rangle, \tag{13}$$

$$\partial_t\delta N-\mathcal{L}_W^0\delta N-\delta\mathcal{L}_W\delta N=\delta\mathcal{L}_W n. \tag{14}$$

On the left-hand side of Eq. (14), we recognize a linear term describing free propagation of the drift waves in the inhomogeneous medium, and a nonlinear term describing wave-wave interactions. The right-hand side is a source term, providing the coupling to the average equation.

The solution strategy is standard: Eq. (14) is first solved by the method of characteristics, and the result is substituted into Eq. (13) in order to obtain a closed equation for the average distribution function, i.e., a *kinetic equation*. The characteristic equations of the wave Liouville equation (14) must be solved backwards in time [27],

$$\frac{d\mathbf{x}(t|t')}{dt'}=\mathbf{V}^g(\mathbf{k}(t|t'))+\overline{\mathbf{V}}(\mathbf{x}(t|t'),t'), \tag{15}$$

$$\frac{d\mathbf{k}(t|t')}{dt'}=\overline{\mathbf{W}}(\mathbf{x}(t|t'),\mathbf{k}(t|t'),t'). \tag{16}$$

The "initial" condition is

$$\mathbf{x}(t|t)=\mathbf{x},\quad \mathbf{k}(t|t)=\mathbf{k}. \tag{17}$$

The solution of these Langevin equations in a given realization is

$$\mathbf{x}(t|t')=\mathbf{x}-\int_{t'}^{t}dt_1\{\mathbf{V}^g(\mathbf{k}(t|t_1))+\overline{\mathbf{V}}(\mathbf{x}(t|t_1),t_1)\},$$
$$\mathbf{k}(t|t')=\mathbf{k}-\int_{t'}^{t}dt_1\overline{\mathbf{W}}(\mathbf{x}(t|t_1),\mathbf{k}(t|t_1),t_1). \tag{18}$$

The solution of the partial differential equation (14) is then

$$\delta N(\mathbf{x},\mathbf{k},t)=\int_0^t dt_1\,\delta\mathcal{L}_W(\mathbf{x}(t|t_1),\mathbf{k}(t|t_1),t_1)\times n(\mathbf{x}(t|t_1),\mathbf{k}(t|t_1),t_1)+\delta N(\mathbf{x}(t|0),\mathbf{k}(t|0),0). \tag{19}$$

For simplicity we assume that at time zero the fluctuation is zero: $\delta N(\mathbf{x},\mathbf{k},0)=0$. Substitution into Eq. (13) yields

$$\partial_t n(\mathbf{x},\mathbf{k},t)-\mathcal{L}_W^0 n(\mathbf{x},\mathbf{k},t)=\int_0^t dt_1\langle\delta\mathcal{L}_W[\mathbf{x},\mathbf{k},t]\,\delta\mathcal{L}_W(\mathbf{x}(t|t_1),\mathbf{k}(t|t_1),t_1)\times n(\mathbf{x}(t|t_1),\mathbf{k}(t|t_1),t_1)\rangle. \tag{20}$$

We obtained a *non-Markovian, nonlocal equation* of the same type as Eq. (27) of Ref. [27]. Note that, although $\delta\mathcal{L}_W$ (10) is a linear combination of $\partial/\partial\mathbf{x}$ and $\partial/\partial\mathbf{k}$, Eq. (20) *is not a diffusion equation*. Indeed, the density profile on the right-hand side is evaluated at $\mathbf{x}(t|t_1),\mathbf{k}(t|t_1)$, which are stochastic quantities [Eq. (18)]. Hence, the factor $n(\mathbf{x}(t|t_1),\mathbf{k}(t|t_1),t_1)$ cannot be taken out of the average. This factor could possibly be expanded into an infinite series of powers of $[\mathbf{x}(t|t_1)-\mathbf{x}]$ and of $[\mathbf{k}(t|t_1)-\mathbf{k}]$, which would involve all partial derivatives of $n(\mathbf{x},\mathbf{k},t)$ and very complicated averages as coefficients. This shows that Eq. (20) describes, in general, a nondiffusive process. The non-Gaussian features mentioned in Sec. I and in Refs. [5] and [16] are presumably hidden in this equation, which is an exact consequence of the wave Liouville equation.

In order to proceed further, we assume as in Ref. [27] that the correlation length $\lambda_\perp$ is much smaller than the macroscopic gradient lengths, L_n, L_{nk}, both in $\mathbf{x}$ and in $\mathbf{k}$. As we are dealing here with large-scale fluctuations, defined by the condition $\langle q\rangle\ \rho_s\ll 1$, this implies the assumption $\rho_s\ll\lambda_\perp\ll L_n,L_{nk}$, which is not unreasonable. This argument allows us to eliminate the delocalization, and use the following approximation in the integrand of Eq. (20): $n(\mathbf{x}(t|t_1),\mathbf{k}(t|t_1),t_1)\approx n[\mathbf{x},\mathbf{k},t_1]$, i.e., the leading term in the expansion mentioned above. The equation thus becomes

$$\partial_t n(\mathbf{x},\mathbf{k},t)-\mathcal{L}_W^0 n(\mathbf{x},\mathbf{k},t)=\int_0^t dt_1\langle\delta\mathcal{L}_W[\mathbf{x},\mathbf{k},t]\times\delta\mathcal{L}_W(\mathbf{x}(t|t_1),\mathbf{k}(t|t_1),t_1)\rangle\ \ n[\mathbf{x},\mathbf{k},t_1]. \tag{21}$$

This is a *closed, non-Markovian equation of evolution for the average distribution function*. Using the definition (10), this equation is written explicitly as follows:

$$\partial_t n(\mathbf{x},\mathbf{k},t)+\mathbf{V}^g(\mathbf{k})\cdot\frac{\partial}{\partial\mathbf{x}}n(\mathbf{x},\mathbf{k},t)=\int_0^t dt_1\Big\{\frac{\partial}{\partial\mathbf{x}}\cdot\overleftrightarrow{\mathsf{L}}^{XX}(t-t_1)\cdot\frac{\partial}{\partial\mathbf{x}}+\frac{\partial}{\partial\mathbf{x}}\cdot\overleftrightarrow{\mathsf{L}}^{XK}(t-t_1)\cdot\frac{\partial}{\partial\mathbf{k}}+\frac{\partial}{\partial\mathbf{k}}\cdot\overleftrightarrow{\mathsf{L}}^{KX}(t-t_1)\cdot\frac{\partial}{\partial\mathbf{x}}+\frac{\partial}{\partial\mathbf{k}}\cdot\overleftrightarrow{\mathsf{L}}^{KK}(t-t_1)\cdot\frac{\partial}{\partial\mathbf{k}}\Big\}n(\mathbf{x},\mathbf{k},t_1). \tag{22}$$

This will be called the (true) *wave kinetic equation*. It is a *non-Markovian "advection-double-diffusion" equation*, describing two coupled diffusion processes, respectively, in **x** space and in **k** space, combined with propagation (advection) in **x** space. Equation (22) contains the precise formulation of what Diamond and his group call the "random walk in **k** space." These authors, however, consider neither the coupling of this process with the diffusion in **x** space, nor the non-Markovian character of these processes. (A similar equation, in the Markovian limit and without the cross-coefficients, thus describing independent diffusion in **x** space and in **k** space, appears in Ref. [15] for the related streamer problem.) The relation between their work and ours will be discussed at the end of this paper.

Equation (22) introduces four 2×2 Lagrangian correlation tensors, defined as follows:

$$\mathsf{L}^{XX}_{r|s}(t-t_1)=\langle \overline{V}_r[\mathbf{x},t]\overline{V}_s(\mathbf{x}(t|t_1),t_1)\rangle, \quad (23)$$

$$\mathsf{L}^{XK}_{r|s}(t-t_1)=\langle \overline{V}_r[\mathbf{x},t]\overline{W}_s(\mathbf{x}(t|t_1),\mathbf{k}(t|t_1),t_1)\rangle, \quad (24)$$

$$\mathsf{L}^{KX}_{r|s}(t-t_1)=\langle \overline{W}_r[\mathbf{x},\mathbf{k},t]\overline{V}_s(\mathbf{x}(t|t_1),t_1)\rangle, \quad (25)$$

$$\mathsf{L}^{KK}_{r|s}(t-t_1)=\langle \overline{W}_r[\mathbf{x},\mathbf{k},t]\overline{W}_s(\mathbf{x}(t|t_1),\mathbf{k}(t|t_1),t_1)\rangle. \quad (26)$$

Assuming stationary turbulence, these functions only depend on the difference of the two times. If Eq. (22) could be set in Markovian form, it would introduce four asymptotic diffusion tensors, defined as usual,

$$\mathsf{D}^{KK}_{r|s}=\int_0^\infty dt\, \mathsf{L}^{KK}_{r|s}(t), \quad (27)$$

with similar definitions for the three other tensors. The Markovian form is, however, not necessarily justified in general [27].

IV. THE DCT METHOD FOR ZONAL FLOWS

An essential role in the nature of strongly turbulent phenomena is played by the trapping processes in the rugged potential landscape. It is therefore natural to study these phenomena by using the idea of the *decorrelation trajectory* (DCT), developed for "ordinary" drift-wave turbulence in Ref. [19]. This method requires an extension, which will be the subject of the present section.

We study the stochastic motion of a drift-wave quasiparticle in the presence of a fluctuating electrostatic potential $\Phi(\mathbf{x},t)$ defined as

$$\Phi(\mathbf{x},t)=\varepsilon\,\phi\left(\frac{\mathbf{x}}{\lambda},\frac{t}{\tau_c}\right), \quad (28)$$

where ε measures the characteristic amplitude of the potential and ϕ is a dimensionless function of the space and time variables. The fluctuations are characterized by a correlation length λ and a correlation time τ_c, such that $\langle\Phi(\mathbf{0},0)\Phi(\mathbf{x},t)\rangle\approx 0$ when $|\mathbf{x}|\gg\lambda$ and/or $t\gg\tau_c$. We use the dimensionless variables $\overline{\mathbf{x}},\overline{\mathbf{k}},\theta$ defined as

$$\mathbf{x}=\lambda\overline{\mathbf{x}},\quad \mathbf{k}=\rho_s^{-1}\overline{\mathbf{k}},\quad t=\tau_c\theta. \quad (29)$$

For simplicity, we will omit the overbar in the forthcoming equations. The Langevin equations of motion of the quasiparticle (15), (16) (in the forward time direction) are

$$\frac{dx(\theta)}{d\theta}=K_d v^g_x(\mathbf{k}(\theta))-K\left.\frac{\partial\phi(x,y,\theta)}{\partial y}\right|_{\mathbf{x}=\mathbf{x}(\theta)}\equiv K_d v^g_x(\mathbf{k}(\theta))+Kv_x(\mathbf{x}(\theta),\theta), \quad (30)$$

$$\frac{dy(\theta)}{d\theta}=K_d v^g_y(\mathbf{k}(\theta))+K\left.\frac{\partial\phi(x,y,\theta)}{\partial x}\right|_{\mathbf{x}=\mathbf{x}(\theta)}\equiv K_d v^g_y(\mathbf{k}(\theta))+Kv_y(\mathbf{x}(\theta),\theta), \quad (31)$$

$$\frac{dk_x(\theta)}{d\theta}=Kk_x(\theta)\left.\frac{\partial^2\phi(x,y,\theta)}{\partial x\partial y}\right|_{\mathbf{x}=\mathbf{x}(\theta)}-Kk_y(\theta)\left.\frac{\partial^2\phi(x,y,\theta)}{\partial x^2}\right|_{\mathbf{x}=\mathbf{x}(\theta)}\equiv Kw_x(\mathbf{x}(\theta),\mathbf{k}(\theta),\theta), \quad (32)$$

$$\frac{dk_y(\theta)}{d\theta}=Kk_x(\theta)\left.\frac{\partial^2\phi(x,y,\theta)}{\partial y^2}\right|_{\mathbf{x}=\mathbf{x}(\theta)}-Kk_y(\theta)\left.\frac{\partial^2\phi(x,y,\theta)}{\partial x\partial y}\right|_{\mathbf{x}=\mathbf{x}(\theta)}\equiv Kw_y(\mathbf{x}(\theta),\mathbf{k}(\theta),\theta). \quad (33)$$

These equations will be solved with the following initial condition:

$$\mathbf{x}(0)=\mathbf{0},\quad \mathbf{k}(0)=\mathbf{k}^0. \quad (34)$$

(It is important to take an initial wave vector of nonzero length: an initial $|\mathbf{k}^0|=0$ would remain zero for all times.) The three scaled velocities $\mathbf{v}^g$, $\mathbf{v}$, and $\mathbf{w}$ are defined by these equations; they are related to the corresponding dimensional quantities as follows:

$$\mathbf{V}^g=\frac{\lambda}{\tau_c}K_d\mathbf{v}^g,\quad \overline{\mathbf{V}}=\frac{\lambda}{\tau_c}K\mathbf{v},\quad \overline{\mathbf{W}}=\frac{1}{\rho_s\tau_c}K\mathbf{w}. \quad (35)$$

We introduced here the two basic dimensionless parameters characterizing the turbulence: the *Kubo number K*, related to the intensity ε of the fluctuations, and the *diamagnetic Kubo number*, related to the gradient length through V_*,

$$K=\frac{\tau_c}{\lambda}\frac{c\varepsilon}{B\lambda}, \quad K_d=\frac{\tau_c}{\lambda}V_*. \tag{36}$$

The components of the dimensionless unperturbed group velocity are

$$v_x^g(\mathbf{k})=-\frac{2k_xk_y}{(1+k_x^2+k_y^2)^2}, \quad v_y^g(\mathbf{k})=\frac{1+k_x^2-k_y^2}{(1+k_x^2+k_y^2)^2}. \tag{37}$$

It should be noted that Eqs. (30)–(33) derive from the time-dependent Hamiltonian (5),

$$\frac{d\mathbf{x}}{d\theta}=\frac{\partial H}{\partial \mathbf{k}}, \quad \frac{d\mathbf{k}}{d\theta}=-\frac{\partial H}{\partial \mathbf{x}}. \tag{38}$$

The transport problem requires the evaluation of the four Lagrangian correlations (23)–(26). We concentrate here on the last one, which introduces all the new features; the three others are treated in a completely similar fashion. Its corresponding dimensionless form, for a homogeneous and stationary turbulent state, is defined as

$$\mathsf{L}_{r|s}^{KK}(t)=\frac{1}{(\rho_s\tau_c)^2}K^2\mathcal{L}_{r|s}^{KK}(t/\tau_c). \tag{39}$$

Using Eq. (26), we obtain

$$\mathcal{L}_{r|s}^{KK}(\theta)=\int d\mathbf{x}\,d\mathbf{k}\langle w_r(\mathbf{0},\mathbf{k}^0,0)w_s(\mathbf{x},\mathbf{k},\theta)\times\delta(\mathbf{x}-\mathbf{x}(\theta))\,\delta(\mathbf{k}-\mathbf{k}(\theta))\rangle. \tag{40}$$

In order to prepare the way for the DCT method, we first note that all fluctuating quantities (including $\mathbf{v}$ and $\mathbf{w}$) are derived from the potential ϕ. As in all theories based on Langevin equations, the primary Eulerian potential autocorrelation has to be specified *a priori*. This quantity is assumed to be of the same form as in Ref. [19],

$$\langle\phi(\mathbf{0},0)\phi(\mathbf{x},\theta)\rangle=\mathcal{E}(\mathbf{x})\mathcal{T}(\theta), \tag{41}$$

where $\mathcal{E}(\mathbf{x})$ is a dimensionless function of the position, with a maximum at the origin, and $\mathcal{T}(\theta)$ is a similar function of time. In the explicit calculations of the next section, we use the following simple forms (Ornstein-Uhlenbeck process):

$$\mathcal{E}(\mathbf{x})=\exp\left(-\frac{x^2+y^2}{2}\right), \quad \mathcal{T}(\theta)=e^{-\theta}, \tag{42}$$

but in the remaining part of the present section, these functions can remain unspecified. We introduce the matrix u_{rs},

$$u_{rs}(\mathbf{x},\theta)=\frac{\partial}{\partial x_r}v_s(\mathbf{x},\theta), \tag{43}$$

such that [see Eqs. (32),(33)]

$$w_r(\mathbf{x},\mathbf{k},\theta)=-k_su_{rs}(\mathbf{x},\theta). \tag{44}$$

We define the notations for the relevant Eulerian correlations,

$$\begin{aligned}
\langle\phi(\mathbf{0},0)v_j(\mathbf{x},\theta)\rangle&=\mathcal{E}_{\phi|j}(\mathbf{x})\mathcal{T}(\theta),\\
\langle v_r(\mathbf{0},0)v_j(\mathbf{x},\theta)\rangle&=\mathcal{E}_{r|j}(\mathbf{x})\mathcal{T}(\theta),\\
\langle u_{rs}(\mathbf{0},0)v_j(\mathbf{x},\theta)\rangle&=\mathcal{E}_{rs|j}(\mathbf{x})\mathcal{T}(\theta),\\
\langle\phi(\mathbf{0},0)u_{jm}(\mathbf{x},\theta)\rangle&=\mathcal{E}_{\phi|jm}(\mathbf{x})\mathcal{T}(\theta),\\
\langle v_r(\mathbf{0},0)u_{jm}(\mathbf{x},\theta)\rangle&=\mathcal{E}_{r|jm}(\mathbf{x})\mathcal{T}(\theta),\\
\langle u_{rs}(\mathbf{0},0)u_{jm}(\mathbf{x},\theta)\rangle&=\mathcal{E}_{rs|jm}(\mathbf{x})\mathcal{T}(\theta).
\end{aligned} \tag{45}$$

All these functions can be derived from the primary potential correlation as follows:

$$\begin{aligned}
&\mathcal{E}_{\phi|x}=-\frac{\partial}{\partial y}\mathcal{E}, \quad \mathcal{E}_{\phi|y}=\frac{\partial}{\partial x}\mathcal{E},\\
&\mathcal{E}_{x|x}=-\frac{\partial^2}{\partial y^2}\mathcal{E}, \quad \mathcal{E}_{y|y}=-\frac{\partial^2}{\partial x^2}\mathcal{E},\\
&\mathcal{E}_{x|y}=\mathcal{E}_{y|x}=\frac{\partial^2}{\partial x\partial y}\mathcal{E},\\
&\mathcal{E}_{rs|j}=-\frac{\partial}{\partial x_r}\mathcal{E}_{s|j}, \quad \mathcal{E}_{\phi|jm}=\frac{\partial}{\partial x_j}\mathcal{E}_{\phi|m},\\
&\mathcal{E}_{r|jm}=\frac{\partial}{\partial x_j}\mathcal{E}_{r|m}, \quad \mathcal{E}_{rs|jm}=\frac{\partial}{\partial x_j}\mathcal{E}_{rs|m},
\end{aligned} \tag{46}$$

We note the following symmetries:

$$\begin{aligned}
&\mathcal{E}_{x|y}=\mathcal{E}_{y|x}, \quad \mathcal{E}_{\phi|xx}=-\mathcal{E}_{\phi|yy},\\
&\mathcal{E}_{xx|xx}=\mathcal{E}_{yy|yy}=-\mathcal{E}_{xx|yy}=-\mathcal{E}_{yy|xx}=-\mathcal{E}_{xy|yx}=-\mathcal{E}_{yx|xy},\\
&\mathcal{E}_{yy|xy}=\mathcal{E}_{xy|yy}=-\mathcal{E}_{xx|xy}=-\mathcal{E}_{xy|xx},\\
&\mathcal{E}_{xx|yx}=\mathcal{E}_{yx|xx}=-\mathcal{E}_{yy|yx}=-\mathcal{E}_{yx|xx}.
\end{aligned} \tag{47}$$

We define some combinations of these Eulerian correlations,

$$H_r=k_n^0\mathcal{E}_{rn|\phi}, \tag{48}$$

$$A_r=k_n\mathcal{E}_{\phi|rn}, \tag{49}$$

$$B_{r|s}=k_n\mathcal{E}_{r|sn}, \tag{50}$$

$$C_{r|s}=k_n^0\mathcal{E}_{rn|s}, \tag{51}$$

$$A_{r|s}=k_m^0k_n\mathcal{E}_{rm|sn}=A_{s|r}. \tag{52}$$

It is useful to note the following identity:

$$A_{r|s}=k_n\frac{\partial}{\partial x_s}C_{r|n}. \tag{53}$$

We denote by a superscript 0 the value of a quantity at the origin, thus $\mathcal{E}^0_{..|..}=\mathcal{E}_{..|..}(\mathbf{x}=\mathbf{0})$, $A^0_r=A_r(\mathbf{x}=\mathbf{0},\mathbf{k}=\mathbf{k}^0)$, etc. Next, we introduce

$$\Delta^0=A^0_{x|x}A^0_{y|y}-(A^0_{x|y})^2, \tag{54}$$

$$D^0=\Delta^0-A^0_{x|x}(A^0_y)^2-A^0_{y|y}(A^0_x)^2+A^0_{x|y}A^0_xA^0_y. \tag{55}$$

The following combinations appear in the final results:

$$\begin{aligned}F^0_x&=A^0_{y|y}A^0_x-A^0_{x|y}A^0_y,\\ F^0_y&=A^0_{x|x}A^0_y-A^0_{x|y}A^0_x,\\ J^0_x&=[A^0_{y|y}-(A^0_y)^2]\Delta^0-A^0_{y|y}A^0_{x|y}A^0_xA^0_y,\\ J^0_y&=[A^0_{x|x}-(A^0_x)^2]\Delta^0-A^0_{x|x}A^0_{x|y}A^0_xA^0_y,\\ L^0&=-A^0_{x|y}\Delta^0+A^0_{x|x}A^0_{y|y}A^0_xA^0_y.\end{aligned} \tag{56}$$

We now develop the extension of the DCT method, following the line of Ref. [19]. The basic step is the decomposition of the ensemble of realizations of the turbulent ensemble into subensembles. This decomposition is now different from the cited one, because not only the potential ϕ and its first derivatives (through $\mathbf{v}$), but also its second derivatives (through $\mathbf{w}$) enter the theory. We therefore define the subensemble S as the set of realizations in which the potential ϕ, the two components of the velocity v_r, and the two components of the "$\mathbf{k}$ velocity" w_r have a given value at time 0,

$$S:\quad \phi(\mathbf{0},0)=\phi^0,\quad v_r(\mathbf{0},0)=v^0_r,\\ -k^0_s u_{rs}(\mathbf{0},0)=w^0_r. \tag{57}$$

Let $P_0(\phi^0,\mathbf{v}^0,\mathbf{w}^0)$ be the probability distribution of these initial values, assumed to be Gaussian. Then the *KK*-Lagrangian correlation (40) is

$$\mathcal{L}^{KK}_{xx}(\theta)=\int d\phi^0 d\mathbf{v}^0 d\mathbf{w}^0 P_0(\phi^0,\mathbf{v}^0,\mathbf{w}^0)\\ \times w^0_x\langle w_x(\mathbf{x}(\theta),\mathbf{k}(\theta),\theta)\rangle^S, \tag{58}$$

where $\langle\ \rangle^S$ denotes the average in the subensemble. Note the important fact that in the Lagrangian correlation in S, $\langle w_x[\mathbf{0},\mathbf{k}^0,0]\ w_x(\mathbf{x}(\theta),\mathbf{k}(\theta),\theta)\rangle^S$, the first factor can be taken out of the average because of Eq. (57), hence the calculation of this quantity is reduced to the simpler calculation of the average Lagrangian velocity. The first goal is the calculation of the distribution function P_0,

$$\begin{aligned}P_0(\phi^0,\mathbf{v}^0,\mathbf{w}^0)&=\langle\delta(\phi^0-\phi(\mathbf{0},0))\delta^2(v^0_m-v_m(\mathbf{0},0))\delta^2(w^0_n+k^0_s u_{ns}(\mathbf{0},0))\rangle\\ &=(2\pi)^{-5}\int ds\,d\mathbf{q}\,d\mathbf{p}\exp(is\phi^0+iq_mv^0_m+ip_nw^0_n)\\ &\quad\times\exp\{-\tfrac{1}{2}[s^2\mathcal{E}^0+q_rq_s\mathcal{E}^0_{r|s}+p_np_mk^0_rk^0_s\mathcal{E}^0_{nr|ms}+2sq_r\mathcal{E}^0_{\phi|r}-2sp_nk^0_r\mathcal{E}^0_{\phi|nr}-2q_rp_nk^0_s\mathcal{E}^0_{r|ns}]\}.\end{aligned} \tag{59}$$

Note that $\mathcal{E}^0=1$, $\mathcal{E}^0_{r|s}=\delta_{rs}$, $\mathcal{E}^0_{\phi|r}=\mathcal{E}^0_{r|ns}=0$. The remaining integrations are elementary, though somewhat tedious:

$$\begin{aligned}P_0(\phi^0,\mathbf{v}^0,\mathbf{w}^0)=\frac{1}{\sqrt{(2\pi)^5D^0}}\exp\Bigg\{-\frac{1}{2}\Bigg[&\frac{\Delta^0}{D^0}(\phi^0)^2+(v^0_x)^2+(v^0_y)^2+\frac{J^0_x}{D^0\Delta^0}(w^0_x)^2+\frac{J^0_y}{D^0\Delta^0}(w^0_y)^2+\frac{2L^0}{D^0\Delta^0}w^0_xw^0_y\\ &+\frac{2F^0_x}{D^0}\phi^0w^0_x+\frac{2F^0_y}{D^0}\phi^0w^0_y\Bigg]\Bigg\}.\end{aligned} \tag{60}$$

The average velocities in the subensemble are obtained by an extension of the method described in Ref. [19]:

$$\langle v_n(\mathbf{x},\theta)\rangle^S=\frac{\langle v_n(\mathbf{x},\theta)\delta(\phi^0-\phi(\mathbf{0},0))\delta^2(v^0_m-v_m(\mathbf{0},0))\delta^2(w^0_r+k^0_su_{rs}(\mathbf{0},0))\rangle}{P_0(\phi^0,\mathbf{v}^0,\mathbf{w}^0)}\equiv v^S_n(\mathbf{x})\mathcal{T}(\theta). \tag{61}$$

A lengthy, but elementary calculation yields

$$\begin{aligned}v^S_n(\mathbf{x})=&\frac{1}{D^0}(\Delta^0\mathcal{E}_{\phi|n}-F^0_xC_{x|n}-F^0_yC_{y|n})\phi^0+\mathcal{E}_{x|n}v^0_x+\mathcal{E}_{y|n}v^0_y+\frac{1}{D^0\Delta^0}(\Delta^0F^0_x\mathcal{E}_{\phi|n}-J^0_xC_{x|n}-L^0C_{y|n})w^0_x\\ &+\frac{1}{D^0\Delta^0}(\Delta^0F^0_y\mathcal{E}_{\phi|n}-L^0C_{x|n}-J^0_yC_{y|n})w^0_y.\end{aligned} \tag{62}$$

The average $\mathbf{k}$ velocity in the subensemble is obtained in the same way,

$$\langle w_n(\mathbf{x},\mathbf{k},\theta)\rangle^S=w^S_n(\mathbf{x},\mathbf{k})\mathcal{T}(\theta), \tag{63}$$

with

$$w_n^S(\mathbf{x},\mathbf{k}) = \frac{1}{D^0}(-\Delta^0 A_n + F_x^0 A_{x|n} + F_y^0 A_{y|n})\phi^0 - B_{x|n}v_x^0 - B_{y|n}v_y^0 + \frac{1}{D^0\Delta^0}(-\Delta^0 F_x^0 A_n + J_x^0 A_{x|n} + L^0 A_{y|n})w_x^0 + \frac{1}{D^0\Delta^0}(-\Delta^0 F_y^0 A_n + L^0 A_{x|n} + J_y^0 A_{y|n})w_y^0. \tag{64}$$

A strong test of these expressions is $v_n^S(\mathbf{0}) = v_n^0$, $w_n^S(\mathbf{0},\mathbf{k}^0) = w_n^0$.

We may also calculate the average potential in the subensemble,

$$\langle \phi(\mathbf{x},\theta)\rangle^S = \phi^S(\mathbf{x},\mathbf{k})\mathcal{T}(\theta) = \left[\frac{1}{D^0}(\Delta^0\mathcal{E} - F_x^0 H_x - F_y^0 H_y)\phi^0 + \mathcal{E}_{x|\phi}v_x^0 + \mathcal{E}_{y|\phi}v_y^0 + \frac{1}{D^0\Delta^0}(\Delta^0 F_x^0\mathcal{E} - J_x^0 H_x - L^0 H_y)w_x^0 + \frac{1}{D^0\Delta^0}(\Delta^0 F_y^0\mathcal{E} - L^0 H_x - J_y^0 H_y)w_y^0\right]\mathcal{T}(\theta). \tag{65}$$

The remaining treatment closely follows Ref. [19]. We define in a given subensemble S a *deterministic decorrelation trajectory* by the equations of motion,

$$\frac{d\mathbf{x}^S(\theta)}{d\theta} = K_d \mathbf{v}^g(\mathbf{k}^S(\theta)) + K\mathbf{v}^S(\mathbf{x}^S(\theta))\mathcal{T}(\theta),$$

$$\frac{d\mathbf{k}^S(\theta)}{d\theta} = K\mathbf{w}^S(\mathbf{x}^S(\theta),\mathbf{k}^S(\theta))\mathcal{T}(\theta),$$

$$\mathbf{x}^S(0) = 0, \quad \mathbf{k}^S(0) = \mathbf{k}^0. \tag{66}$$

These equations determine the motion of a fictitious quasiparticle along the deterministic DCT. We note that the Hamiltonian structure of the starting equations (38) is inherited by the DCT equations. Indeed, defining an average Hamiltonian in the subensemble,

$$H^S(\mathbf{x}^S,\mathbf{k}^S,\theta) = K_d\omega_d(\mathbf{k}^S) + K\mathbf{k}^S\cdot\mathbf{v}^S(\mathbf{x}^S)\mathcal{T}(\theta), \tag{67}$$

it is easily checked that Eqs. (66) can be written as

$$\frac{d\mathbf{x}^S}{d\theta} = \frac{\partial H^S}{\partial \mathbf{k}^S}, \quad \frac{d\mathbf{k}^S}{d\theta} = -\frac{\partial H^S}{\partial \mathbf{x}^S}. \tag{68}$$

It follows from this structure that, in the stationary case $[\mathcal{T}(\theta)=1]$, the Hamiltonian is a constant of the motion along the DCT,

$$H^S(\mathbf{x}^S(\theta),\mathbf{k}^S(\theta)) = H^S(\mathbf{0},\mathbf{k}^0). \tag{69}$$

The deterministic DCT is now introduced in the expressions of the four Lagrangian correlation functions (23)–(26) [see Eq. (58)]. These quantities, evaluated in the *decorrelation trajectory approximation,* are

$$\mathcal{L}_{j|n}^{XX}(\theta) = \int d\phi^0 d\mathbf{v}^0 d\mathbf{w}^0 P_0(\phi^0,\mathbf{v}^0,\mathbf{w}^0) v_j^0 v_n^S(\mathbf{x}^S(\theta),\theta)\mathcal{T}(\theta),$$

$$\mathcal{L}_{j|n}^{XK}(\theta) = \int d\phi^0 d\mathbf{v}^0 d\mathbf{w}^0 P_0(\phi^0,\mathbf{v}^0,\mathbf{w}^0) \times v_j^0 w_n^S(\mathbf{x}^S(\theta),\mathbf{k}^S(\theta),\theta)\mathcal{T}(\theta),$$

$$\mathcal{L}_{j|n}^{KX}(\theta) = \int d\phi^0 d\mathbf{v}^0 d\mathbf{w}^0 P_0(\phi^0,\mathbf{v}^0,\mathbf{w}^0) \times w_j^0 v_n^S(\mathbf{x}^S(\theta),\theta)\mathcal{T}(\theta),$$

$$\mathcal{L}_{j|n}^{KK}(\theta) = \int d\phi^0 d\mathbf{v}^0 d\mathbf{w}^0 P_0(\phi^0,\mathbf{v}^0,\mathbf{w}^0) \times w_j^0 w_n^S(\mathbf{x}^S(\theta),\mathbf{k}^S(\theta),\theta)\mathcal{T}(\theta). \tag{70}$$

We stress again the great advantage of the DCT approximation: the calculation of the Lagrangian correlations is replaced by the simpler problem of the calculation of an Eulerian average, evaluated along the deterministic decorrelation trajectory. The present problem is, however, significantly more complicated in the present case than for the simple drift-wave turbulence treated in Ref. [19]. The complication comes from the intimate coupling of the equations for $\mathbf{x}^S(\theta)$ and $\mathbf{k}^S(\theta)$. Any attempt to treat separately one or the other variable would be a gross oversimplification. The Lagrangian correlations are now fivefold integrals, which makes their evaluation more difficult. The final result depends on more parameters, viz., the Kubo number K, the diamagnetic Kubo number K_d, but also the initial wave vector $\mathbf{k}^0$. The numerical calculation of the Lagrangian correlations and of the diffusion coefficients will be the object of a forthcoming work. Some important qualitative features can, however, be obtained from an analysis of the individual DCT trajectories.

V. THE DECORRELATION TRAJECTORIES

We now consider the result of the numerical integration of the decorrelation trajectories (66). For definiteness, we assume the form (41),(42) for the Eulerian potential autocorrelation. A specified trajectory depends on the five parameters

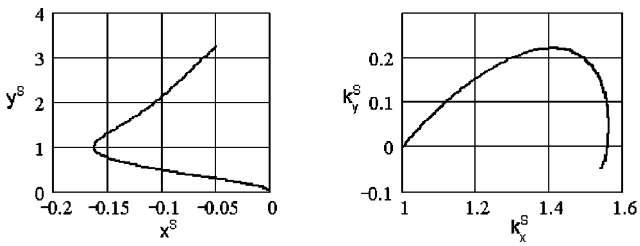

FIG. 1. Decorrelation trajectories (y^S-x^S) and (k_y^S-k_x^S) for $K=0.5$. Subensemble parameters: $\phi^0=2$, $v_x^0=v_y^0=0$, $w_x^0=w_y^0=1$. $K_d=1$. Initial wave vector: $k_x^0=1$, $k_y^0=0$.

defining the subensemble S ($\phi^0,\mathbf{v}^0,\mathbf{w}^0$) and on the initial value of the wave vector $\mathbf{k}^0$, as well as on the two dimensionless Kubo numbers K and K_d. For the purpose of illustration, we choose the case of a subensemble with a relatively high value of $\phi^0=2$. Although the weight of the corresponding trajectories is rather small in the expression of the correlation functions [because of the factor P_0 in Eqs. (70)], the qualitative features of the DCT are more clearly exhibited in this extreme case. We thus define the subensemble S by the following values of the parameters: $\phi^0=2$, $v_x^0=v_y^0=0$, $w_x^0=w_y^0=1$. We also choose the fixed value $K_d=1$. The choice $\mathbf{v}^0=\mathbf{0}$ implies that the (fictitious) quasiparticle starts at time zero with the initial group velocity $K_d\mathbf{v}^g(\mathbf{k}^0)$ and ends after a sufficiently long time ($\theta\gg\theta_{\mathrm{tr}}$), when $v_n^S=0$, $w_n^S=0$, with the final group velocity $K_d\mathbf{v}^g(\mathbf{k}^{as})$. Note that, because of the factorization property $\langle\mathbf{v}(\mathbf{0},0)\mathbf{v}(\mathbf{x},\theta)\rangle^S=\mathbf{v}^0\langle\mathbf{v}(\mathbf{x},\theta)\rangle^S$ (and similarly for $\mathbf{w}$) [see Eq. (58)], the vanishing of $\mathbf{v}^S,\mathbf{w}^S$ implies the vanishing of the Lagrangian velocity correlation in the subensemble S. Thus the *trapping time* θ_{tr} is the time after which the fictitious quasiparticle is no longer correlated along its trajectory with its initial value. The trapping time θ_{tr} is determined numerically from the shape of the trajectories (see below). It should be clear that θ_{tr} relates to a single DCT. (Note that a characteristic time related to trapping is defined in Ref. [29] as $\theta_b^{-1}=\omega_b=[q^2v(\mathbf{q})\ k_\theta|dv^g(\mathbf{k})/dk_r|]^{1/2}$; this is the bounce frequency of a drift plasmon trapped by zonal flow in k_r space. It is not clear that this is the same as our θ_{tr} defined above.) The initial wave vector is chosen as $k_x^0=1$, $k_y^0=0$. As a result, the (unperturbed) group velocity at the initial time is $\mathbf{v}^g(\mathbf{k}^0)=(1/2)\ \mathbf{e}_y$. Thus, in the absence of turbulence ($K=0$), the fictitious quasiparticle moves in a straight line in the y direction, with a group velocity that is constant because the wave vector $\mathbf{k}$ remains constant.

We now consider a rather small value of the Kubo number, $K=0.5$. Figure 1 shows the corresponding DCT trajectories, and Fig. 2 shows the position $\mathbf{x}^S(\theta)$ and the wave vector $\mathbf{k}^S(\theta)$ as functions of time. In Fig. 3, the corresponding graphs of the velocities $\mathbf{v}^S(\theta)$ in $\mathbf{x}$ space [together with the group velocity $\mathbf{v}^g(\theta)$] and $\mathbf{w}^S(\theta)$ in $\mathbf{k}$ space are shown.

Even in this relatively weak turbulence, the picture departs radically from the unperturbed motion. The beginning of a *trapping process in* $\mathbf{x}$ *space* is evident: the (fictitious) quasiparticle starts with the initial group velocity $\mathbf{v}^g(\mathbf{k}^0)$, but the turbulent velocity quickly overcomes the latter and deflects the particle from its rectilinear motion. The turbulent

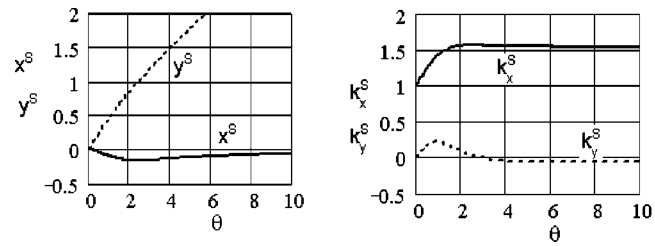

FIG. 2. DCT trajectories: position $\mathbf{x}^S(\theta)$ and wave vector $\mathbf{k}^S(\theta)$ as functions of time, for $K=0.5$.

component of the velocity $\mathbf{v}^S$ vanishes after a time that will be called the *trapping time* θ_{tr}, of order of the correlation time; in the present case its value is seen to be $\theta_{\mathrm{tr}}\approx 3$, after which the quasiparticle moves again uniformly, with the group velocity. Meanwhile, the group velocity has changed because the wave vector has changed. Thus the quasiparticle is deflected from its unperturbed motion in the y direction and moves now in an oblique direction. We thus witness here a *refraction phenomenon* due to the passage through the turbulent medium. This refraction effect is also found (in a different context) in Refs. [15] and [16].

The wave vector starts from $\mathbf{k}^0$ and initially increases in both directions, the growth being largest in the x ("radial") direction. Note that the increase of k_x^S is monotonous, until it reaches a saturation value after $\theta\approx\theta_{\mathrm{tr}}$. The y ("poloidal") component k_y^S quickly reaches a maximum: its monotonous growth is then stopped and reversed after a certain time ($\theta\approx 1$). It then changes sign, and finally ($\theta\approx\theta_{\mathrm{tr}}$) it reaches a negative saturation value. This is the manifestation of the *trapping process in* $\mathbf{k}$ *space*, which only affects (in the present situation) the y component. This process ends after $\theta\approx\theta_{\mathrm{tr}}$, after which $\mathbf{k}^S$ remains constant: $\mathbf{k}^S(\theta)\to\mathbf{k}^\infty$ [and $\mathbf{w}^S(\theta)\to\mathbf{0}$]. It is important to note that (in the present case) $|k_y^\infty|<k_x^\infty$ ($k_x^\infty=1.54, k_y^\infty=-0.047$). As a result, in the asymptotic state ($\theta>\theta_{\mathrm{tr}}$), the average length scale of the turbulence in the radial direction is much smaller than in the poloidal direction. This obviously explains the fragmentation

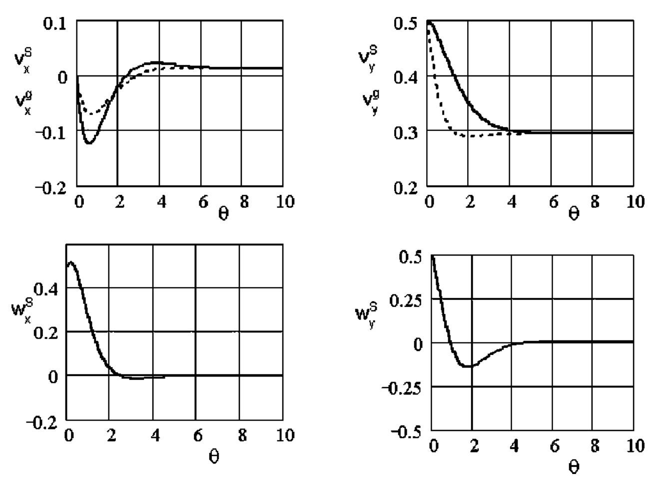

FIG. 3. Complete DCT velocities $\mathbf{V}^S(\theta)=\mathbf{v}^g(\mathbf{k}(\theta))+K\mathbf{v}^S(\theta)$ in $\mathbf{x}$ space and $\mathbf{w}^S(\theta)$ in $\mathbf{k}$ space, as functions of time, for $K=0.5$. The dashed lines represent the group velocity $\mathbf{v}^g[\mathbf{k}^S(\theta)]$.

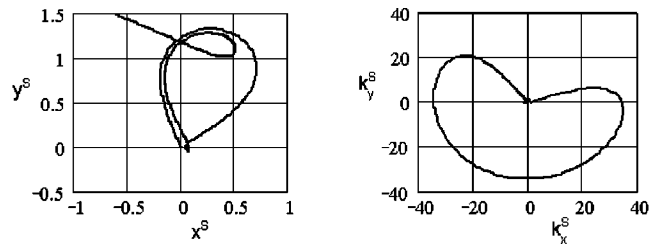

FIG. 4. Decorrelation trajectories (y^S-x^S) and (k_y^S-k_x^S) for $K=10$. Subensemble parameters: $\phi^0=2$, $v_x^0=v_y^0=0$, $w_x^0=w_y^0=1$. $K_d=1$. Initial wave vector: $k_x^0=1$, $k_y^0=0$.

process described qualitatively in the first section, and implies the *generation of a* ($small$-k_y) *zonal flow*.

To sum up: during the trapping time $\theta_{\rm tr}$, the wave vector changes from its initial value to a constant asymptotic value with $|k_y^\infty|<|k_x^\infty|$; the quasiparticle is trapped during that time, and ends up moving with a new, deflected group velocity (*refraction*). In the final state, the length scale of the turbulence in the y (poloidal) direction is much greater than in the x (radial) direction.

This analysis shows that the decorrelation process is now richer than in the case studied in Ref. [19]. In particular, the position and the wave vector move in a strictly coupled way and cannot be considered separately from each other. There is weak trapping in $\mathbf{x}$ space, but the trapping of the k_y wave-vector component is already quite significant at this relatively modest value of the Kubo number ($K=0.5$).

We now consider a situation of strong turbulence, $K=10$, with the same subensemble parameters. The DCT position and the wave vector of the fictitious quasiparticle are shown in Figs. 4 and 5, and the corresponding velocities are shown in Fig. 6.

The features which were merely sketched in the case $K=0.5$ are now greatly enhanced. The (fictitious) quasiparticle is clearly *strongly trapped in* $\mathbf{x}$ *space*: its motion is a ''broken oscillation'' during the time $\theta_{\rm tr}$ (which has barely changed, $\theta_{\rm tr}\approx 3$). During the trapping time it is more and more strongly deflected. Its trajectory makes two turns, thus confining the quasiparticle to a finite region of space. But after $\theta_{\rm tr}$, the turbulent component of the velocity vanishes, and the fictitious quasiparticle moves away with the final group velocity $[v_x^g(\mathbf{k}^\infty)=-0.232, v_y^g(\mathbf{k}^\infty)=0.115]$. Meanwhile, both the k_x^S and the k_y^S components of the wave vector undergo a broken oscillation which stops at $\theta\approx\theta_{\rm tr}$, when they reach the values $k_x^\infty=0.879$, $k_y^\infty=0.965$. We thus witness

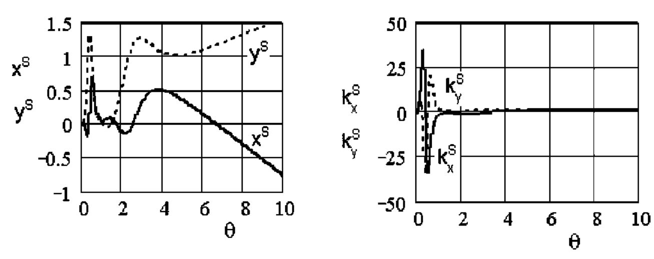

FIG. 5. DCT trajectories: position $\mathbf{x}^S(\theta)$ and wave vector $\mathbf{k}^S(\theta)$ as functions of time, for $K=10$.

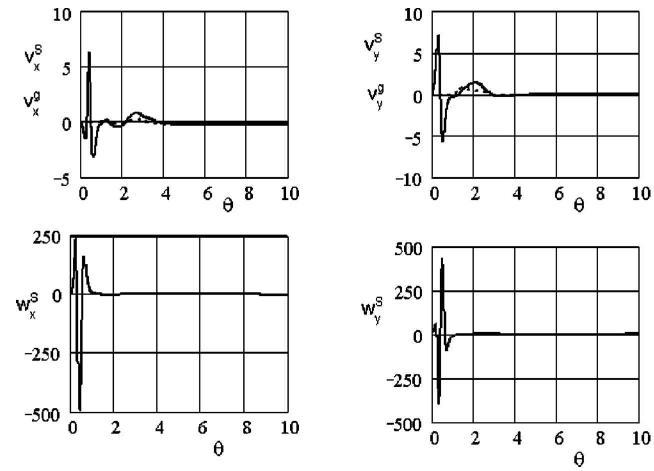

FIG. 6. Complete DCT velocities $\mathbf{V}^S(\theta)$ and $\mathbf{w}^S(\theta)$ as functions of time, for $K=10$. The dashed lines represent the group velocity $\mathbf{v}^g(\mathbf{k}^S(\theta))$.

strong trapping in both $\mathbf{k}$ *directions*. In the present situation we can no longer speak of zonal flow generation: k_y^∞ is now of order 1, and moreover it surpasses k_x^∞ in absolute value. The strong turbulence produces in this case a fragmentation both in the radial and in the poloidal directions.

In order to obtain a more global insight, we plotted in Fig. 7 the asymptotic wave-vector components (k_x^∞, k_y^∞) against the Kubo number K for given subensemble parameters (in particular, $\phi^0=1.5$). It clearly appears that true zonal flow generation is possible only in a limited range of Kubo numbers. In the present subensemble, the two criteria $|k_y^\infty|<|k_x^\infty|$, $|k_y^\infty|<1$ are satisfied in the range $0<K\lesssim 1.5$. Beyond this range, k_y^∞ performs an oscillation (in K) and finally settles at an absolute value larger than 1. k_x^∞ has a similar behavior, but is shifted with respect to the former. This shift explains the smallness of the ratio $|k_y^\infty|/|k_x^\infty|$ for small K (zonal flow generation).

Clearly, the present discussion refers to a single subensemble; a more complete scanning of the parameter space is necessary for a firm general conclusion. We have considered

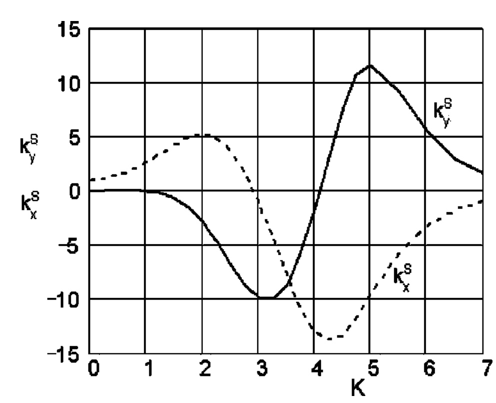

FIG. 7. Asymptotic poloidal and radial components of the wave vector, k_y^∞, k_x^∞ vs Kubo number K. Subensemble parameters: $\phi^0=1.5$, $v_x^0=v_y^0=0$, $w_x^0=w_y^0=1$. $K_d=1$. Initial wave vector: $k_x^0=1$, $k_y^0=0$.

other values of ϕ^0 and found very similar behavior. The corresponding curves are dilated (for smaller ϕ^0) or contracted (for larger ϕ^0) in the K direction.

In conclusion, it clearly appears that the trapping of the quasiparticles (i.e., of the drift wave packets) plays a major role in their dynamics, even at relatively small levels of turbulence (e.g., $K=0.5$). Thus, the quasilinear approximation is hardly valid. The trapping process will have a strong influence on the diffusion coefficients. Their quasilinear approximation certainly gives an overestimated value.

VI. THE DIAMOND MODEL

As stated in the Introduction, Diamond and co-workers [13,15] were the first authors who introduced the idea of a ''random walk in **k** space'' for explaining the generation of transport barriers. We now analyze the nature of their model and study it in light of the DCT method.

A. The Diamond *D*-2 model

A first approximation in Ref. [5] is *the neglect of the turbulence in the motion of the quasiparticles*, i.e., in the equations for $x(\theta),y(\theta)$. Indeed, the only trace of the particle motion in [5] is the appearance of the (deterministic) group velocity V^g in the quasilinear propagator defining the diffusion coefficient in **k** space. The resulting equations for the DCT in this ''Diamond-2 model'' (which is different from the original Diamond model) are then Eqs. (66), in which the term $K\mathbf{v}^S[\mathbf{x}^S(\theta)]\mathcal{T}(\theta)$ is omitted.

The DCT trajectories of this model were compared with the ones of the ''complete'' model (66). For brevity, we shall not, however, illustrate the results in detail. Let us just mention that for weak turbulence (e.g., $K=0.5$) the trajectory of $\mathbf{k}(\theta)$ is not very different from that of the complete model, except that it stops at a rather different asymptotic value; as a result, the final motion in **x** space is incorrectly predicted. For strong turbulence the discrepancy is much worse.

B. The Diamond *D*-1 model

We discuss in some more detail a comparison with the final model used in Ref. [5]. In that paper a further simplifying approximation is made, by assuming that *the potential depends only on the x coordinate*: $\phi(x,t)$. This could be called a ''pseudo-one-dimensional model,'' denoted by *D*-1. It is not truly one-dimensional because, as will be seen below, the motion in **x** space is two-dimensional, although the motion in **k** space is indeed one-dimensional.

In order to compare the *D*-1 model to the complete DCT approximation, the latter has to be reconsidered from the beginning, because many quantities vanish for a one-dimensional potential. The starting Langevin equations (30)–(33) now reduce to

$$\frac{dx(\theta)}{d\theta}=K_d v_x^g(k_x(\theta),k_y^0),$$

$$\frac{dy(\theta)}{d\theta}=K_d v_y^g(k_x(\theta),k_y^0)+K\frac{\partial\phi[x,\theta]}{\partial x}\bigg|_{x=x(\theta)}$$

$$\equiv K_d v_y^g(k_x(\theta),k_y^0)+Kv_y(x(\theta),\theta),$$

$$\frac{dk_x(\theta)}{d\theta}=-Kk_y^0\frac{\partial^2\phi[x,\theta]}{\partial x^2}\bigg|_{x=x(\theta)}\equiv Kw_x(x(\theta),k_y^0,\theta),$$

$$\frac{dk_y(\theta)}{d\theta}=0. \tag{71}$$

The component k_y of the wave vector thus remains constant. It should, however, not be put equal to zero, otherwise the k_x component would also remain constant, and there would be no ''random walk in **k** space.'' The variable k_x component appears only in the group velocity. The three nontrivial equations remain coupled. The only turbulent velocity components that remain in this case are v_y and u_x. The *D*-1 model assumes that $Kv_y(x(\theta),\theta)$ can be neglected.

We now note that for this ''one-dimensional potential'' many Eulerian correlations vanish; the only nonzero ones are $\mathcal{E}_{\phi|y}$, $\mathcal{E}_{\phi|xy}$, $\mathcal{E}_{y|y}$, $\mathcal{E}_{y|xy}$, $\mathcal{E}_{xy|y}$, and $\mathcal{E}_{xy|xy}$. The subensemble S is now defined by the constraints

$$S:\quad \phi(0,0)=\phi^0,\quad v_y(0,0)=v_y^0,\quad -k_y^0u_{xy}(0,0)=w_x^0. \tag{72}$$

The calculations of the various DCT quantities must be redone along the same lines as in Eqs. (59)–(65). Thus, the probability distribution of the initial values is

$$P_0(\phi^0,v_y^0,w_x^0)$$
$$=\langle\delta(\phi^0-\phi(0,0))\delta(v_y^0-v_y(0,0))\delta(w_x^0+k_y^0u_{xy}(0,0))\rangle$$
$$=\frac{1}{[(2\pi)^3G^0]^{1/2}}\exp\left\{-\frac{1}{2}\left[\frac{A_{x|x}^0}{G^0}(\phi^0)^2+(v_y^0)^2+\frac{1}{G^0}(w_x^0)^2+\frac{A_x^0}{G^0}\phi^0w_x^0\right]\right\}, \tag{73}$$

where

$$G^0=A_{x|x}^0-(A_x^0)^2. \tag{74}$$

The average quantities in the subensemble are

$$v_y^S(x,k_y^0)=\frac{1}{G^0}(A_{x|x}^0\mathcal{E}_{\phi|y}-A_x^0C_{x|y})\phi^0+\mathcal{E}_{y|y}v_y^0+\frac{1}{G^0}(A_x^0\mathcal{E}_{\phi|y}-C_{x|y})w_x^0, \tag{75}$$

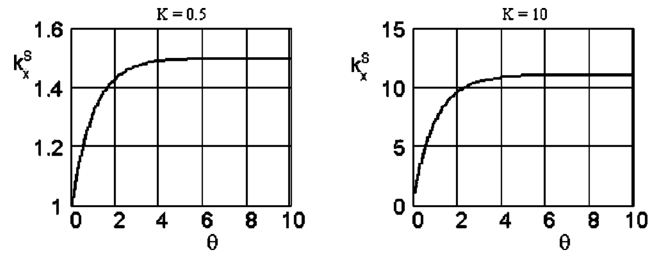

FIG. 8. DCT wave vector $k_x^S(\theta)$ as a function of time, for two values of K, for both the complete pseudo-one-dimensional model and the D-1 model. The two curves are exactly superposed. Subensemble parameters: $\phi^0=2$, $v_y^0=0$, $w_x^0=1$. $K_d=1$. Initial wave vector: $k_x^0=1$, $k_y^0=0.1$.

$$w_x^S(x,k_y^0)=\frac{1}{G^0}(-A_{x|x}^0A_x+A_x^0A_{x|x})\phi^0-B_{y|x}v_y^0$$

$$+\frac{1}{G^0}(-A_x^0A_x+A_{x|x})w_x^0. \tag{76}$$

The equations of motion for the DCT are

$$\frac{dx^S(\theta)}{d\theta}=K_dv_x^g(k_x^S(\theta),k_y^0),$$

$$\frac{dy^S(\theta)}{d\theta}=K_dv_y^g(k_x^S(\theta),K_y^0)+Kv_y^S(x^S(\theta),k_y^0)\mathcal{T}(\theta),$$

$$\frac{dk_x^S(\theta)}{d\theta}=Kw_x^S(x^S(\theta),k_y^0)\mathcal{T}(\theta),$$

$$\frac{dk_y^S(\theta)}{d\theta}=0,$$

$$x^S(0)=y^S(0)=0,\quad k_x^S(0)=k_x^0,\quad k_y^S(0)=k_y^0. \tag{77}$$

These equations define the "complete" pseudo-one-dimensional DCT. The Diamond D-1 model is obtained by setting $v_y^S(x^S(\theta),k_y^0)=0$ in the second equation (77). The peculiar structure of the one-dimensional model has an interesting consequence. The equations for $x^S(\theta)$ and for $k_x^S(\theta)$ form a closed set. Upon substituting their solution into the equation for $y^S(\theta)$, the latter is found by a mere quadrature. The same remark holds for the original Langevin equations (71). As a result, if one is only interested in the evolution of the wave vector (as in Ref. [5]), the neglect of the turbulence in dy^S/dt has no consequence: the wave vector $k_x^S(\theta)$, and also $x^S(\theta)$, obtained in the complete pseudo-one-dimensional model or in the D-1 model are the same. But, of course, the two-dimensional spatial DCT $\mathbf{x}^S(\theta)$ will be different in the two models. This is shown in Figs. 8 and 9.

We first note that the wave vector $k_x^S(\theta)$ increases sharply and monotonously during a time $\theta\approx4$, after which it saturates at a constant asymptotic value. This means that *there is no trapping* in $\mathbf{k}$ in this model. As for the y^S-x^S DCT orbits, they are different in the two models, as expected. The transient effect of the turbulence is just a shift, followed by a

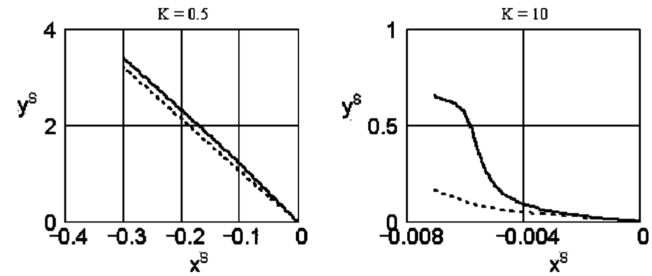

FIG. 9. DCT orbits in the x^S-y^S plane for two values of K. Solid line, complete one-dimensional model; dashed line, D-1 model.

regular motion (with velocity $\mathbf{v}^g$). In particular, *no trapping effect appears in these models, even at relatively high levels of turbulence, where the two-dimensional DCT's show a strong trapping effect* (see Figs. 2 and 5). Note that even the "Diamond D-2 model" exhibits trapping. Thus, in the one-dimensional models a very important feature of the turbulence is lost.

Next, we note that the one-dimensional models do describe the radial fragmentation process of the drift-wave structures by the increase of $k_x^S(\theta)$, but they do not *generate* a zonal flow. Indeed, $k_y(\theta)$ remains constant in these models [see Eqs. (71), (77)]. The poloidal zonal flow is prescribed externally in the models with $\phi(x,\theta)$ independent of y. It thus appears that a two-dimensional model is indispensable for covering the full physics of the process.

VII. CONCLUSIONS

In the present work we treated in detail the process called "*random walk in wave-vector space*" by Diamond and coworkers [13,5]. This leads to an alternative view of the formation of transport barriers in a turbulent plasma. Rather than basing the study on a dispersion relation and the related modulational instability [30], we consider a picture based on the evolution of a set of drift-wave packets ("quasiparticles"). The formation of zonal flows appears as a result of the fragmentation of the wave packets in the radial direction and the generation of long-wavelength structures in the poloidal direction.

The evolution of the distribution function of these packets is described by a well-known Liouville equation, deriving from a Hamiltonian. Assuming that the system is in a turbulent state, an application of the standard methods of nonequilibrium statistical mechanics [26,27] leads, in general, to a nondiffusive equation, responsible for non-Gaussian behavior. If the spatial delocalization is neglected, a true wave kinetic equation, i.e., a closed equation for the ensemble-averaged part of the distribution function, is obtained. The new feature here is the form of this non-Markovian advection-diffusion equation: it describes the strongly coupled diffusive processes in $\mathbf{x}$ space and in $\mathbf{k}$ space. General expressions of the four diffusion tensors are derived in terms of Lagrangian correlation functions of the ($\mathbf{x}$ and $\mathbf{k}$) velocities.

The evaluation of such Lagrangian correlations is a well-known stumbling block in turbulence theories. We showed that the quasilinear approximation is very much limited to very weak turbulence, because it neglects the important trapping effect. The latter appears to be quite important in both **x** and **k** spaces. In order to take account of this effect, we used the decorrelation trajectory approximation, which was recently developed precisely for this purpose. Its generalization to the present problem produces analytical expressions for the Lagrangian correlations and the diffusion coefficients. The numerical evaluation of these coefficients is, however, postponed to a forthcoming paper.

The analysis of typical individual decorrelation trajectories in a given subensemble (and for a given form of the Eulerian potential autocorrelation) provides us with a vivid illustration of the trapping processes. In particular, it explains the radial fragmentation of the wave packets, as well as the generation of long-wavelength zonal flows. The latter is, however, only produced in a limited range of Kubo numbers, whose extension depends on the subensemble parameters. A comparison has been made with previously used models. Of course, the picture is not yet complete. These effects must be averaged over all subensembles, i.e., over all initial conditions of the potential and of the velocities, in the calculation of the observable diffusion coefficients. As stated above, this will be the subject of a forthcoming work.

ACKNOWLEDGMENTS

We gratefully acknowledge very fruitful discussions with M. Vlad, I. Petrisor, M. Negrea, and J. Misguich.

[1] W. Horton, B. Hu, J. Q. Dong, and P. Zhu, New J. Phys. **5**, 14 (2003).
[2] X. Garbet, Plasma Phys. Controlled Fusion **43**, A251 (2001).
[3] F. Wagner *et al.*, Phys. Rev. Lett. **49**, 1408 (1982).
[4] P. Terry, Rev. Mod. Phys. **72**, 109 (2000).
[5] P. H. Diamond, S. Champeaux, M. Malkov, A. Das, I. Gruzinov, M. N. Rosenbluth, C. Holland, B. Wecht, A. Smolyakov, F. L. Hinton, Z. Lin, and T. S. Hahm, Nucl. Fusion **41**, 1067 (2001).
[6] K. Itoh, S.-I. Itoh, and A. Fukuyama, *Transport and Structural Formation in Plasmas* (Institute of Physics, Bristol, 1999).
[7] S.-I. Itoh and Y. Kawai, *Bifurcation Phenomena in Plasma* (Kyushu University Press, Fukuoka, 2002).
[8] A. Yoshizawa, S-I. Itoh, and K. Itoh, *Plasma and Fluid Turbulence, Theory and Modelling* (Institute of Physics, Bristol, 2003).
[9] Z. Lin, T. S. Hahm, W. W. Lee, W. M. Tang, and R. B. White, Science **281**, 1835 (1998).
[10] H. Biglari, P. H. Diamond, and P. Terry, Phys. Fluids B **2**, 1 (1990).
[11] P. H. Diamond and Y. B. Kim, Phys. Fluids B **3**, 1626 (1991).
[12] S. B. Korsholm, P. K. Michelsen, V. Naulin, J. J. Rasmussen, L. Garcia, B. A. Carreras, and V. E. Lynch, Plasma Phys. Controlled Fusion **43**, 1377 (2001).
[13] P. H. Diamond, M. N. Rosenbluth, F. L. Hinton, M. Malkov, J. Fleischer, and A. Smolyakov, *Proceedings of the 17th IAEA Conference on Fusion Energy, Yokohama* (IAEA, Vienna, 1998), p. IAEA-CN-69/TH3/1.
[14] A. I. Smolyakov, P. H. Diamond, and M. Malkov, Phys. Rev. Lett. **84**, 491 (2000).
[15] P. H. Diamond and M. Malkov, Phys. Scr., T **T98**, 63 (2002).
[16] P. Kaw, R. Singh, and P. H. Diamond, Plasma Phys. Controlled Fusion **44**, 51 (2002).
[17] R. H. Kraichnan, Phys. Fluids **13**, 22 (1970).
[18] J. A. Crottinger and T. H. Dupree, Phys. Fluids B **4**, 2854 (1992).
[19] M. Vlad, F. Spineanu, J. H. Misguich, and R. Balescu, Phys. Rev. E **58**, 7359 (1998).
[20] M. Vlad, F. Spineanu, J. H. Misguich, and R. Balescu, Phys. Rev. E **63**, 066304 (2001).
[21] M. Vlad, F. Spineanu, J. H. Misguich, and R. Balescu, Phys. Rev. E **67**, 026406 (2003).
[22] W. D. McComb, *The Physics of Fluid Turbulence* (Clarendon, Oxford, 1992).
[23] J.-D. Reuss and J. H. Misguich, Phys. Rev. E **54**, 1857 (1996); J.-D. Reuss, M. Vlad, and J. H. Misguich, Phys. Lett. A **241**, 94 (1998).
[24] L. D. Landau and E. M. Lifshitz, *Electrodynamics of Continuous Media* (Pergamon, London, 1951).
[25] T. H. Stix, *Waves in Plasmas* (American Institute of Physics, New York, 1992).
[26] R. Balescu, *Statistical Dynamics: Matter out of Equilibrium* (Imperial College Press, London, 1997).
[27] R. Balescu, Plasma Phys. Controlled Fusion **42**, B1 (2000).
[28] R. Balescu, H.-D. Wang, and J. Misguich, Phys. Plasmas **1**, 3826 (1994).
[29] V. S. Marchenko, Phys. Rev. Lett. **89**, 185002 (2002).
[30] K. Hallatschek and P. H. Diamond, New J. Phys. **5**, 29.1 (2003).